

Anti-Drude Metal of Bosons

Guido Masella,¹ Nikolay V. Prokof'ev,^{2,1} and Guido Pupillo¹

¹*ISIS (UMR 7006) and icFRC, University of Strasbourg and CNRS, 67000 Strasbourg, France*

²*Department of Physics, University of Massachusetts, Amherst, Massachusetts 01003, USA*

(Dated: February 5, 2022)

In the absence of frustration, interacting bosons in the ground state exist either in the superfluid or insulating phases. Superfluidity corresponds to frictionless flow of the matter field, and in optical conductivity is revealed through a distinct δ -functional peak at zero frequency with the amplitude known as the Drude weight. This characteristic low-frequency feature is instead absent in insulating phases, defined by zero static optical conductivity. Here we demonstrate that bosonic particles in disordered one dimensional, $d = 1$, systems can also exist in a conducting, non-superfluid, phase when their hopping is of the dipolar type, often viewed as short-ranged in $d = 1$. This phase is characterized by finite static optical conductivity, followed by a broad anti-Drude peak at finite frequencies. Off-diagonal correlations are also unconventional: they feature an integrable algebraic decay for arbitrarily large values of disorder. These results do not fit the description of any known quantum phase and strongly suggest the existence of a novel conducting state of bosonic matter in the ground state.

Quantum phases of matter are distinguished by their static and dynamical properties, quantified by correlation functions. For interacting bosonic matter in one dimension, the superfluid phase is characterized by a non-integrable algebraic decay of static one-body (off-diagonal) correlations as a function of distance and by a δ -functional peak at zero frequency in the optical conductivity, respectively. The latter is reflecting a singular response to a weak externally applied field. Strong enough disorder can induce a quantum phase transition from the superfluid to an insulating phase, known as the Bose glass [1]. In this phase, off-diagonal correlations decay exponentially with distance and the optical conductivity starts from zero at zero-frequency, reflecting the absence of long-lived collective modes at low-energy. These two phases exhaust the known possibilities for disordered bosons in one dimension in the absence of frustration, where by frustration we understand a situation when the path-integral representation of quantum statistics in imaginary time is not sign-positive. In this work, we provide numerical evidence for the existence of a novel disorder-induced phase that is neither superfluid nor insulating. Despite featuring an algebraic decay of off-diagonal correlations, it has zero superfluid density and its optical conductivity is finite at zero frequency. The latter is followed by a broad peak at a finite frequency of the order of the nearest-neighbor hopping energy. Because of this characteristic "anti-Drude" behavior of optical conductivity, with finite minimum instead of maximum at zero frequency, we term this novel phase an anti-Drude metal of bosons (aDMB).

The aDMB phase is a result of interplay between interactions, disorder, and particle hopping, which we choose to be of the dipolar type. The latter is usually considered as short-ranged in $d = 1$ [2]. For non-interacting models with short-range hopping, disorder is generally expected to localize all wave-functions exponentially (Anderson lo-

calization) [3]. However, recent theoretical works have demonstrated that single particle states can localize algebraically in the presence of couplings that decay with distance as a power-law [4–8]. What happens in strongly interacting systems remained an open question, and this work provides the first answers with the discovery of the aDMB ground state.

Dipolar couplings have been already experimentally realized for internal excitations of cold magnetic atoms [9–12], Rydberg excited atoms [13–15], ions [16, 17], and molecules [18]. The propagation of excitations with dipolar couplings in the presence of disorder is also highly relevant for a variety of solid-state systems, including nuclear spins [19], nitrogen-vacancy centers in diamonds [20], or two-level emitters placed near a photonic crystal waveguide [21].

We note that the existence of a metallic bosonic phase has been suggested previously [22–24]; e.g., in the context of finite-temperature strange metal behavior of high-temperature superconductors [23, 25] and as a possible ground state in lattice models with multi-particle interactions [24, 26, 27]. However, up to date, the existence of a metallic phase of bosons has not been confirmed by exact methods in any physical system. Since frustrated spin systems featuring a variety of spin-liquids phases can be always re-formulated in terms of strongly interacting bosons, we exclude frustrated models from this discussion.

We consider the following Hamiltonian for hard-core bosons confined to one dimension

$$\mathcal{H} = -t \sum_{i < j} \frac{a^3}{|r_{ij}|^3} [b_i^\dagger b_j + \text{H.c.}] + \sum_i \epsilon_i n_i, \quad (n_i \leq 1). \quad (1)$$

We employ standard notations for bosonic creation and annihilation operators on site i and occupation numbers, $n_i = b_i^\dagger b_i$, that cannot exceed unity in the allowed Fock states. The nearest-neighbor hopping amplitude, t , and

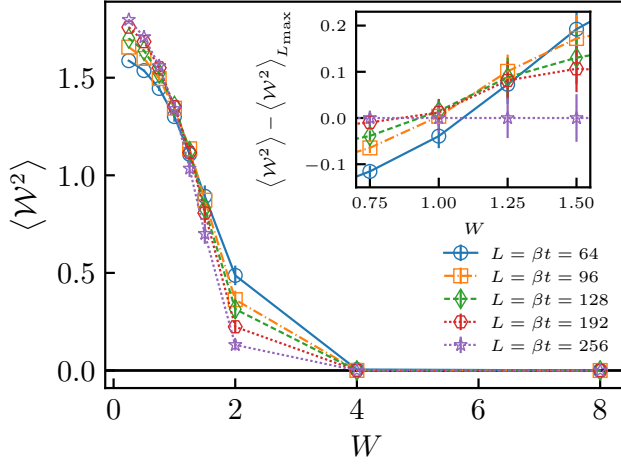


FIG. 1. Mean-squared winding numbers $\langle \mathcal{W}^2 \rangle$ as functions of the disorder strength W for lattice sizes $L = 64$ (blue circles), 96 (orange squares), 128 (green diamonds), 192 (red hexagons), 256 (purple stars). Inset highlights the area near the phase transition, showing crossing points between the curves within the interval $W_c = 1.00 \pm 0.15$; the curve corresponding to the largest size ($L = 256$) is subtracted from all data for clarity.

the lattice spacing, a , are taken as units of energy and length, respectively. Hopping amplitudes between sites i and j decay with the distance between them as r_{ij}^{-3} , and ϵ_i are random on-site energies uniformly distributed between $-W$ and W . In spin language, Eq. (1) is equivalent to an XY Hamiltonian with dipolar couplings, which, in the absence of disorder, can be realized in experiments with cold polar molecules [18], trapped ions [16, 17] and Rydberg atoms [13, 14, 28], with the latter also in the presence of disorder [15]. Recent theoretical works provide strong evidence that Eq. (1) supports a many-body localized (MBL) phase at finite energy [18, 29–32]. Our result then implies that the MBL transition out of aDMB takes place as the temperature is increased. In a system with an upper bound on the maximal energy per particle this result is not that surprising [33].

In the following, we determine the ground-state quantum phases of Eq. (1) using large scale path-integral quantum Monte-Carlo simulations based on the Worm algorithm [34]. Without loss of generality, we focus on particle density $\rho = 1/2$.

For nearest-neighbor hopping only, one-dimensional hard-core bosons behave as spinless fermions and bosonic exchange has to involve all particles in the liquid. A regular system would have finite superfluid density, ρ_s , that characterizes the response to twisted boundary condition caused by an external vector potential field. It can be conveniently computed within quantum Monte-Carlo, see Methods, through the statistics of

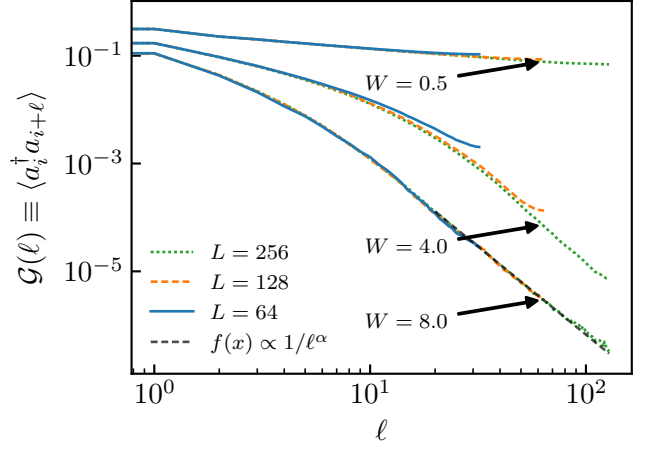


FIG. 2. One-body density matrix $\mathcal{G}(\ell)$ as a function of the distance ℓ for different system sizes $L = 64$ (blue solid lines), 128 (yellow dashed lines), and 256 (green dotted lines), and values of the disorder strength $W = 0.5, 4.0$, and 8.0 (top to bottom). Data is shown on the doubly logarithmic scale. The gray dashed line corresponds to a fit $1/\ell^\alpha$ with $\alpha = 3.26(2)$ of the large distances behaviour for $L = 256$ and $W = 8.0$.

winding numbers, \mathcal{W} , using the Pollock-Ceperley relation $\rho_s \propto \langle \mathcal{W}^2 \rangle$ [35][36]. However, it is well known that the superfluid density of this system is immediately suppressed by any finite strength of disorder W , due to Anderson localization [1]. Dipolar hopping changes this picture entirely, by allowing for pair-wise bosonic exchanges, somewhat similar to soft-core particles. One then expects superfluidity to be robust against weak disorder, and, possibly, undergo a quantum phase transition to a non-superfluid phase when disorder exceeds some critical value W_c .

Figure 1 shows numerical results for the statistics of mean-squared winding numbers $\langle \mathcal{W}^2 \rangle$ as a function of the disorder strength W for different lattice sizes L . Mean-squared winding numbers are expected to be scale invariant at a continuous phase transition, regardless of the system dimension. This allows one to identify the critical disorder strength W_c where superfluidity is lost by the crossing point of the $\langle \mathcal{W}^2 \rangle$ -vs- W curves for different values of L . The figure shows that all sizes larger than $L > 64$ cross at $W_c = 1.00 \pm 0.15$ (see Inset), signalling the transition from a superfluid phase for $W < W_c$ to a quantum phase that is not superfluid for $W > W_c$. In the following, we focus on characterising the properties of this non-superfluid phase with $W > W_c$ by studying its correlation functions and optical conductivity.

The one-body density matrix $\mathcal{G}(\ell) = \langle b_i^\dagger b_{i+\ell} \rangle$ is expected to decay algebraically as a function of distance

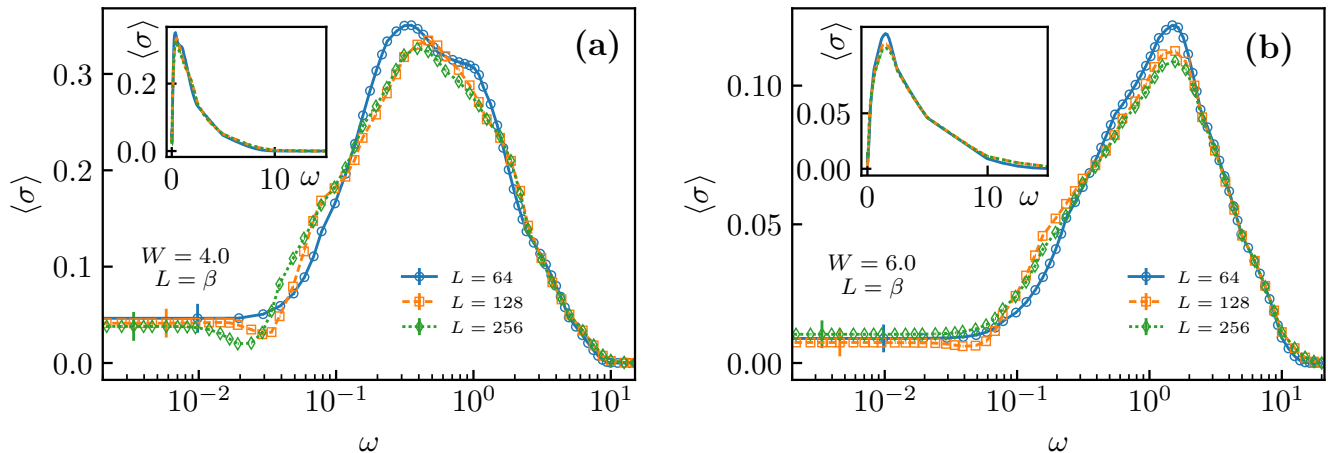


FIG. 3. Disorder-averaged optical conductivity σ as a function of the frequency ω for $W = 4$ (Panel a, left) and $W = 6$ (Panel b, right), at different system sizes $L = 64$ (blue circles), 128 (orange squares), and 256 (green diamonds). Data in the main plots is shown on the logarithmic scale for the frequency, highlighting the behaviour for small ω . Insets show data on the linear scale.

ℓ for a one-dimensional superfluid ground state, while in an insulating phase it is expected to decay exponentially, e.g. in a crystalline phase or Bose glass. Figure 2 shows $\mathcal{G}(\ell)$ for the Hamiltonian Eq. (1), for chosen values of the disorder strength W . The figure shows that in the superfluid phase with $W = 0.5 < W_c$, $\mathcal{G}(\ell)$ displays a slow algebraic decay, as expected. Surprisingly, we find that an initial exponential decay of $\mathcal{G}(\ell)$ is followed at large distances ℓ by an algebraic decay in the non-superfluid phase for $W > W_c$. The large-distance decay is well described by the $\mathcal{G}(\ell) \sim 1/\ell^3$ dependence. This behavior is at odds with known results for insulating many-body phases with short-range hopping [1], indicating that other physical properties may also be unconventional. We thus proceed with analysing the optical conductivity of the non-superfluid phase at $W > W_c$.

The optical conductivity $\sigma(\omega)$ relates the current density J to the strength of an externally applied electric field \mathcal{E} as $J(\omega) = \sigma(\omega)\mathcal{E}(\omega)$, with ω the field frequency. We obtain the optical conductivity $\sigma(\omega)$ within the linear response theory by first computing the current-current correlation function $\chi(i\omega_n) = \langle j(\tau)j(0) \rangle_{i\omega_n}$ at Matsubara frequencies $\omega_n = 2\pi nT$ using the Worm algorithm, followed by its numerical analytic continuation (see Methods). Here j is the lattice current operator defined as $j = it \sum_{i<j} r_{ij} [b_i^\dagger b_j - b_j^\dagger b_i] / r_{ij}^3$.

Figure 3 shows typical examples of the optical conductivity, averaged over a minimum of 384 disorder realizations, as a function of frequency for two values of $W > W_c$ deep in the non-superfluid phase and different lattice sizes L . Consistently with the absence of superfluidity, the figure shows that the characteristic δ -functional peak at zero frequency peak in $\sigma(\omega \simeq 0)$

is absent. However, the numerical results also show two striking features: (i) The zero-frequency response is finite and system size independent within the (relative large) error bars; (ii) Unlike in usual conductors featuring a Drude peak (maximum at $\omega = 0$), the optical conductivity has a minimum at zero frequency followed by a large peak at frequency $\omega \simeq t$, which provides a large response at energies of the order of the nearest-neighbor hopping amplitude. This peak broadens with increasing W , providing a large response up to frequencies $\omega \simeq 10t$. These results for the averaged conductivity demonstrate the existence of a conducting, non superfluid phase of bosons in the ground state. This conducting behaviour is not due to well defined delocalized quasiparticle states as in typical Drude-type metals; rather, it is an "anti-Drude metal", where the largest response occurs at a small but finite frequency.

Figure 4(a) shows selected results for $\sigma(\omega)$ in the aDMB phase for individual realizations of disorder, i.e. without averaging. We find that at frequencies $\omega > t$ the optical conductivity behavior is rather robust and sample-to-sample fluctuations are not substantial. The same cannot be said about the low-frequency part that wildly fluctuates from sample to sample - whilst some of the samples are metallic, the majority display an insulating behavior. This suggests that static σ is in fact not a self-averaging quantity in our system. These fluctuations will be reflected in similar fluctuations in experiments.

The discovery of the aDMB phase is particularly surprising as the dipolar hopping term in Eq. (1) is usually considered to be short ranged in one dimension.

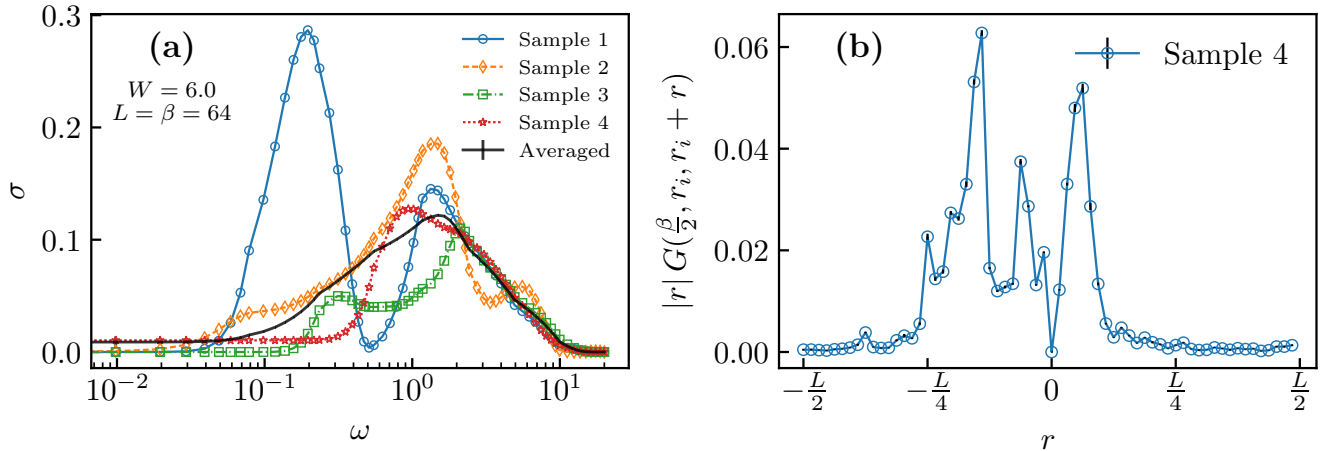


FIG. 4. Panel a: Optical conductivity σ as a function of the frequency ω for different disorder realizations. The black continuous line represents the average over all 384 disordered samples. Panel b: Correlation function $|r| \mathcal{G}_{\tau=\frac{\beta}{2}}(r_i, r_i + r)$ as a function of r , sampled for imaginary time difference $\tau = \frac{\beta}{2}$ between the two end points on the trajectory. Here, r_i is chosen so that $\mathcal{G}_{\frac{\beta}{2}}(r_i, r_i)$ is maximum. This quantity allows one to visualize the main contributions to the current for a single disorder realization when the particle starts from point r_i (see main text and Methods). In both panels data is shown for $L = \beta = 64$ and $W = 6$.

Nevertheless, it leads to large de-localized contributions to the current that can be visualized as follows. The single particle propagator $\mathcal{G}_\tau(r, r') = \langle b_{r'}^\dagger(\tau) b_r(0) \rangle$ encodes information for where a particle/hole injected into the system at site r can go in time τ (for hard core bosons points r and r' are connected by a trajectory). By setting $\tau = \beta/2$ and taking the limit $\beta \rightarrow \infty$ we gain insight into properties of the ground state wave function. Since current operator between distant sites involves an additional power of distance we multiply $\mathcal{G}_{\frac{\beta}{2}}(r, r')$ by $|r - r'|$ to establish a quantitative measure for current contributions. Figure 4(b) visualizes the correlation function $|r| \mathcal{G}_{\frac{\beta}{2}}(r_i, r_i + r)$ for a single conducting realization as a function of the distance r for a fixed value of r_i that was chosen from the condition of maximum for $\mathcal{G}_{\frac{\beta}{2}}(r_i, r_i)$. The figure makes it clear that large current contributions are present over a wide range of distances of the order of $\sim L/4$.

In summary, we have demonstrated that bosonic particles can exist in a unusual metallic phase at zero temperature. It emerges from interplay between disorder, interactions, and dipolar hopping that has already been realized in experiments with Rydberg atoms, cold ions, and polar molecules. These results open many new research directions. These include investigations of new metallic phases that can exist in higher dimensions and possible connections to the experimentally observed “bad metal” states on the finite-temperature phase diagram of high-temperature superconductors.

Acknowledgements – The authors acknowledge sup-

port from the University of Strasbourg Institute of Advanced Studies (USIAS). G. P. acknowledges additional support from the Institut Universitaire de France (IUF) and LABEX CSC. N. P. acknowledges support from the MURI Program “New Quantum Phases of Matter” from AFOSR. Computing time was provided by the High Performance Computing Center of the University of Strasbourg. Part of the computing resources were funded by the Equipex EquipMeso project (Programme Investissements d’Avenir) and the CPER Alsacalcul/Big Data.

-
- [1] T. Giamarchi, *Quantum Physics in One Dimension* (Oxford University Press, 2003).
 - [2] T. Lahaye, C. Menotti, L. Santos, M. Lewenstein, and T. Pfau, The physics of dipolar bosonic quantum gases, *Reports on Progress in Physics* **72**, 126401 (2009).
 - [3] P. W. Anderson, Absence of Diffusion in Certain Random Lattices, *Physical Review* **109**, 1492 (1958).
 - [4] T. Botzung, D. Vodola, P. Naldesi, M. Müller, E. Ercolessi, and G. Pupillo, Algebraic localization from power-law couplings in disordered quantum wires, *Physical Review B* **100**, 155136 (2019).
 - [5] X. Deng, V. E. Kravtsov, G. V. Shlyapnikov, and L. Santos, Duality in Power-Law Localization in Disordered One-Dimensional Systems, *Physical Review Letters* **120**, 110602 (2018).
 - [6] P. A. Nosov, I. M. Khaymovich, and V. E. Kravtsov, Correlation-induced localization, *Physical Review B* **99**, 104203 (2019).
 - [7] F. A. B. F. de Moura, A. V. Malyshev, M. L. Lyra, V. A. Malyshev, and F. Domínguez-Adame, Localization properties of a one-dimensional tight-binding model

- with nonrandom long-range intersite interactions, *Physical Review B* **71**, 174203 (2005).
- [8] G. L. Celardo, R. Kaiser, and F. Borgonovi, Shielding and localization in the presence of long-range hopping, *Physical Review B* **94**, 144206 (2016).
 - [9] A. de Paz, A. Sharma, A. Chotia, E. Maréchal, J. H. Huckans, P. Pedri, L. Santos, O. Gorceix, L. Vernac, and B. Laburthe-Tolra, Nonequilibrium Quantum Magnetism in a Dipolar Lattice Gas, *Physical Review Letters* **111**, 185305 (2013).
 - [10] S. Baier, M. J. Mark, D. Petter, K. Aikawa, L. Chomaz, Z. Cai, M. Baranov, P. Zoller, and F. Ferlaino, Extended Bose-Hubbard models with ultracold magnetic atoms, *Science* **352**, 201 (2016).
 - [11] S. Lepoutre, J. Schachenmayer, L. Gabardos, B. Zhu, B. Naylor, E. Maréchal, O. Gorceix, A. M. Rey, L. Vernac, and B. Laburthe-Tolra, Out-of-equilibrium quantum magnetism and thermalization in a spin-3 many-body dipolar lattice system, *Nature Communications* **10**, 1714 (2019).
 - [12] A. Patscheider, B. Zhu, L. Chomaz, D. Petter, S. Baier, A.-M. Rey, F. Ferlaino, and M. J. Mark, Controlling dipolar exchange interactions in a dense three-dimensional array of large-spin fermions, *Physical Review Research* **2**, 023050 (2020).
 - [13] D. Barredo, H. Labuhn, S. Ravets, T. Lahaye, A. Browaeys, and C. S. Adams, Coherent Excitation Transfer in a Spin Chain of Three Rydberg Atoms, *Physical Review Letters* **114**, 113002 (2015).
 - [14] A. P. Orioli, A. Signoles, H. Wildhagen, G. Günter, J. Berges, S. Whitlock, and M. Weidemüller, Relaxation of an Isolated Dipolar-Interacting Rydberg Quantum Spin System, *Physical Review Letters* **120**, 063601 (2018).
 - [15] S. de Léséleuc, V. Lienhard, P. Scholl, D. Barredo, S. Weber, N. Lang, H. P. Büchler, T. Lahaye, and A. Browaeys, Observation of a symmetry-protected topological phase of interacting bosons with Rydberg atoms, *Science* **365**, 775 (2019).
 - [16] P. Richerme, Z.-X. Gong, A. Lee, C. Senko, J. Smith, M. Foss-Feig, S. Michalakakis, A. V. Gorshkov, and C. Monroe, Non-local propagation of correlations in quantum systems with long-range interactions, *Nature* **511**, 198 (2014).
 - [17] P. Jurcevic, B. P. Lanyon, P. Hauke, C. Hempel, P. Zoller, R. Blatt, and C. F. Roos, Quasiparticle engineering and entanglement propagation in a quantum many-body system, *Nature* **511**, 202 (2014).
 - [18] B. Yan, S. A. Moses, B. Gadway, J. P. Covey, K. R. A. Hazzard, A. M. Rey, D. S. Jin, and J. Ye, Observation of dipolar spin-exchange interactions with lattice-confined polar molecules, *Nature* **501**, 521 (2013).
 - [19] G. A. Álvarez, D. Suter, and R. Kaiser, Localization-delocalization transition in the dynamics of dipolar-coupled nuclear spins, *Science* **349**, 846 (2015).
 - [20] G. Waldherr, Y. Wang, S. Zaiser, M. Jamali, T. Schulte-Herbrüggen, H. Abe, T. Ohshima, J. Isoya, J. F. Du, P. Neumann, and J. Wrachtrup, Quantum error correction in a solid-state hybrid spin register, *Nature* **506**, 204 (2014).
 - [21] C.-L. Hung, A. González-Tudela, J. I. Cirac, and H. J. Kimble, Quantum spin dynamics with pairwise-tunable, long-range interactions, *Proceedings of the National Academy of Sciences* **113**, E4946 (2016).
 - [22] M. V. Feigelman, V. B. Geshkenbein, L. B. Ioffe, and A. I. Larkin, Two-dimensional Bose liquid with strong gauge-field interaction, *Physical Review B* **48**, 16641 (1993).
 - [23] P. Phillips and D. Dalidovich, The Elusive Bose Metal, *Science* **302**, 243 (2003).
 - [24] O. I. Motrunich and M. P. A. Fisher, d -wave correlated critical Bose liquids in two dimensions, *Physical Review B* **75**, 235116 (2007).
 - [25] C. Yang, Y. Liu, Y. Wang, L. Feng, Q. He, J. Sun, Y. Tang, C. Wu, J. Xiong, W. Zhang, X. Lin, H. Yao, H. Liu, G. Fernandes, J. Xu, J. M. Valles, J. Wang, and Y. Li, Intermediate bosonic metallic state in the superconductor-insulator transition, *Science* **366**, 1505 (2019).
 - [26] H.-C. Jiang, M. S. Block, R. V. Mishmash, J. R. Garrison, D. N. Sheng, O. I. Motrunich, and M. P. A. Fisher, Non-Fermi-liquid d -wave metal phase of strongly interacting electrons, *Nature* **493**, 39 (2013).
 - [27] M. S. Block, D. N. Sheng, O. I. Motrunich, and M. P. A. Fisher, Spin Bose-Metal and Valence Bond Solid Phases in a Spin- $1/2$ Model with Ring Exchanges on a Four-Leg Triangular Ladder, *Physical Review Letters* **106**, 157202 (2011).
 - [28] J. Zeiher, J.-y. Choi, A. Rubio-Abadal, T. Pohl, R. van Bijnen, I. Bloch, and C. Gross, Coherent Many-Body Spin Dynamics in a Long-Range Interacting Ising Chain, *Physical Review X* **7**, 041063 (2017).
 - [29] A. L. Burin, Localization in a random XY model with long-range interactions: Intermediate case between single-particle and many-body problems, *Physical Review B* **92**, 104428 (2015).
 - [30] A. L. Burin, Many-body delocalization in a strongly disordered system with long-range interactions: Finite-size scaling, *Physical Review B* **91**, 094202 (2015).
 - [31] A. Safavi-Naini, M. L. Wall, O. L. Acevedo, A. M. Rey, and R. M. Nandkishore, Quantum dynamics of disordered spin chains with power-law interactions, *Physical Review A* **99**, 033610 (2019).
 - [32] X. Deng, G. Masella, G. Pupillo, and L. Santos, Universal Algebraic Growth of Entanglement Entropy in Many-Body Localized Systems with Power-Law Interactions, *Physical Review Letters* **125**, 010401 (2020).
 - [33] Y. Kagan and L. A. Maksimov, Quantum diffusion of atoms in a crystal localization and phonon-stimulated delocalization, *Physics Letters A* **95**, 242 (1983).
 - [34] N. V. Prokof'ev, B. V. Svistunov, and I. S. Tupitsyn, Exact, complete, and universal continuous-time worldline Monte Carlo approach to the statistics of discrete quantum systems, *Journal of Experimental and Theoretical Physics* **87**, 310 (1998).
 - [35] E. L. Pollock and D. M. Ceperley, Path-integral computation of superfluid densities, *Physical Review B* **36**, 8343 (1987).
 - [36] See Supplementary material.
 - [37] B. V. Svistunov, E. Babaev, and N. V. Prokof'ev, *Superfluid States of Matter*, 1st ed. (CRC Press, 2015).
 - [38] R. Levy, J. P. F. LeBlanc, and E. Gull, Implementation of the maximum entropy method for analytic continuation, *Computer Physics Communications* **215**, 149 (2017).
 - [39] N. V. Prokof'ev and B. V. Svistunov, Spectral analysis by the method of consistent constraints, *JETP Letters* **97**, 649 (2013).
 - [40] O. Goulko, A. S. Mishchenko, L. Pollet, N. Prokof'ev,

and B. Svistunov, Numerical analytic continuation: Answers to well-posed questions, *Physical Review B* **95**, 014102 (2017).

- [41] M. Jarrell and J. E. Gubernatis, Bayesian inference and the analytic continuation of imaginary-time quantum Monte Carlo data, *Physics Reports* **269**, 133 (1996).

METHODS

We perform quantum Monte Carlo simulations of Hamiltonian Eq. (1) in the path-integral representation in the grand-canonical ensemble using the worm algorithm [34] for system sizes as large as $L = 256$ and temperatures as low as $T/t = 1/256$. At half-filling, we shift disorder realizations to ensue that $\langle W_i \rangle = \mu = 0$ for each realization, with μ the chemical potential. The resulting density is then $\langle \rho \rangle = \frac{1}{2}$ when averaged over the disorder realizations with tiny, i.e. 2.8% for $L = 256$ and $W = 6.0$, sample-to-sample fluctuations.

In the presence of a constant vector potential Eq. (1) is modified by phase factors in the hopping elements of the form $t_{ij} \rightarrow e^{i\phi r_{ij}}$. An expansion of the phase factor up to the second order in ϕ leads to the current operator for the studied Hamiltonian

$$j = it \sum_{i < j} \frac{r_{ij}}{|r_{ij}|^3} [b_i^\dagger b_j - b_j^\dagger b_i] \quad (2)$$

along with the additional operator \mathcal{T} that is required for proper definition of the current-current correlation function (see below)

$$\mathcal{T} = -t \sum_{i < j} \frac{r_{ij}^2}{|r_{ij}|^3} [b_i^\dagger b_j + b_j^\dagger b_i]. \quad (3)$$

The superfluid stiffness is, as usual, defined as the response of the free energy F to a weak externally applied phase ϕ

$$\Upsilon_s = L \left. \frac{\partial^2 F(\phi)}{\partial \phi^2} \right|_{\phi=0}, \quad (4)$$

which in quantum Monte Carlo calculations is directly computed as [35, 37]

$$\Upsilon_s = L \langle \mathcal{W}^2 \rangle, \quad (5)$$

with \mathcal{W} the path winding number. In the case of hopping connecting distant sites, as in Eq. (1), \mathcal{W} can be written as $\mathcal{W} = N_{\rightarrow} - N_{\leftarrow} = \sum_k r_k$ with N_{\Leftarrow} the number of particle trajectories crossing the hypothetical boundary of the system in a given direction, and with the sum going over all the hopping elements in a single worldline configuration of the entire system (here, r_k represents the displacement between the sites connected by the k -th hopping event).

Current-current correlation functions In the regime of weak field ϕ (linear response) it is sufficient to look at the current-current correlation function

$$\chi(\omega_n) = \langle j(\tau)j(0) \rangle_{\omega_n} \quad (6)$$

at Matsubara frequencies $\omega_n = 2\pi Tn$ ($n > 0$). We compute it numerically and perform an analytic continuation procedure to obtain the conductivity $\sigma(\omega)$. Here,

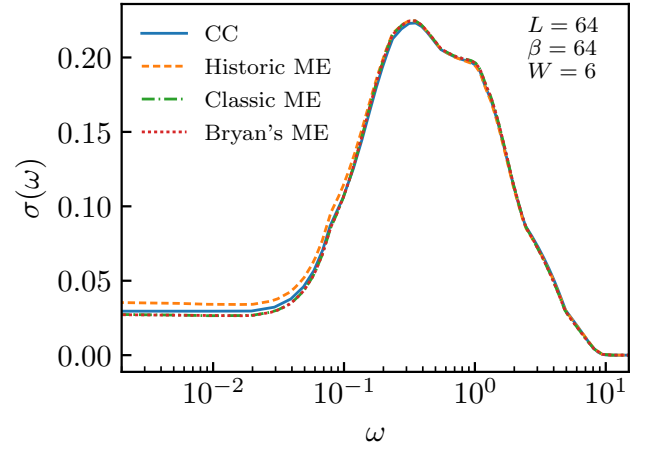


FIG. 5. Averaged optical conductivity σ as a function of the frequency ω for different analytic continuation algorithms including, consistent constraints (solid blue), and three different variants of the maximum entropy method: historic (dashed yellow), classic (dash dotted green), and Bryan's method (dotted red) [see [38]]. Data is shown for $L = \beta = 64$ and $W = 6$. The average is taken over all 384 disordered samples.

the subscript ω_n denotes that the Fourier transform is taken of the corresponding correlation function $\langle j(\tau)j(0) \rangle$ in imaginary time. Path integral representation of quantum statistics for the Hamiltonian Eq. (1) allows one to sample Fourier components of this correlation function directly, and collect statistics for different Matsubara frequencies by using the estimator $|\sum_k ir_k e^{i\omega_n \tau_k}|^2$, where again the sum goes over all hopping transitions on the systems worldlines. For zero-frequency $\omega_n = 0$, this estimator is equivalent to measuring the winding number squared \mathcal{W}^2 while for large Matsubara frequencies it approaches the constant value corresponding to the estimator for \mathcal{T} . After computing statistical averages, we subtract $\langle \mathcal{T} \rangle$ from the data to obtain the current-current correlation function. To suppress finite size effects associated with rare configurations with finite winding numbers, we restrict the sampling of the correlation function $\chi(\omega_n)$ to configurations $\mathcal{W} = 0$.

Analytic continuation Here, we are interested in computing the optical conductivity $\sigma(\omega)$, an observable that can be measured experimentally but not readily accessible by numerical techniques. By the dissipation-fluctuation theorem

$$\chi(\omega_n) = -\frac{2}{\pi} \int_0^\infty \frac{\omega^2}{\omega_n^2 + \omega^2} \sigma(\omega) d\omega. \quad (7)$$

Finding $\sigma(\omega)$ is thus a standard ill conditioned inverse problem when small fluctuations of the input due to statistical noise in the Monte Carlo sampling lead to large fluctuations in the output results. To solve this problem we use a method of consistent constraints [39, 40]. It allows us to restore the spectral density $\sigma(\omega)$ from the

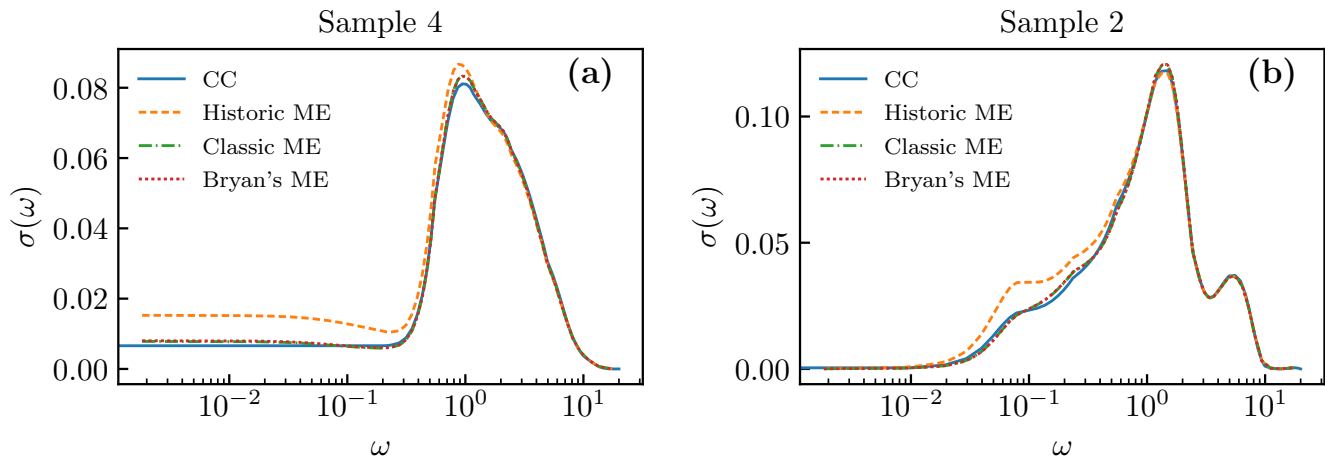


FIG. 6. Comparison of different analytic continuation algorithms for single disorder realizations for the optical conductivity $\sigma(\omega)$ in a system with $L = 64$ and $\beta = 64$. Each panel corresponds to different disorder realizations and different lines to different algorithms including, consistent constraints (solid blue), and three different maxent variants: historic (dashed yellow), classic (dash dotted green), and Bryan's method (dotted red) [see [38]].

corresponding correlation function $\chi(i\omega_n)$.

As a consistency check we compare our results for the analytic continuation of our data with a standard implementation [38] of the maximum entropy method [41]. We note that maxent suffers from numerical instabilities due to small errors on our data in Matsubara frequency domain and it is able to find acceptable solutions only when artificially increasing the errors and using the solutions found with the method of consistent constraints

as “default model”. The comparison is shown in Fig. 5 in the case of the disorder-averaged conductivity and in Fig. 6 for single disorder realizations. Here, three different solutions are shown for maxent (ME), corresponding to the three different variations of the maximum entropy method available in the implementation of Ref.[38] (historic, classic and Bryan's method). We see that, with exception of the historic variant, all the solutions are essentially identical to each other and our solution is accepted by maxent with little or no modifications.